

Note

## Almond shell xylo-oligosaccharides exhibiting immunostimulatory activity

Debora Nabarlatz,<sup>a,\*</sup> Daniel Montané,<sup>a</sup> Alžbeta Kardošová,<sup>b</sup> Slávka Bekešová,<sup>b</sup>  
Věra Hříbalová<sup>c</sup> and Anna Ebringerová<sup>b</sup>

<sup>a</sup>Department of Chemical Engineering, ETSEQ, Rovira i Virgili University, Avinguda dels Països Catalans 26,  
E-43007 Tarragona, Catalunya, Spain

<sup>b</sup>Department of Glycomaterials, Institute of Chemistry, Slovak Academy of Sciences, Dúbravská cesta 9, 845 38 Bratislava, Slovakia

<sup>c</sup>National Institute of Public Health, Šrobárová 48, 100 42 Prague, Czech Republic

Received 3 November 2006; received in revised form 1 February 2007; accepted 16 February 2007

Available online 23 February 2007

**Abstract**—Partially O-acetylated xylo-oligosaccharides (DXO) isolated from almond shells by autohydrolysis as well as their de-acetylated form (DeXO) were subjected to chemical, molecular, and structural analyses. They represent a mixture of neutral and acidic oligomers and low-molecular weight polymers related to (4-O-methyl-D-glucurono)-D-xylan. DXO and DeXO showed direct mitogenic activity and enhancement of the T-mitogen-induced proliferation of rat thymocytes, indicating the immunostimulatory potential of the almond shell xylo-oligosaccharides.

© 2007 Elsevier Ltd. All rights reserved.

**Keywords:** Almond shells; Xylo-oligosaccharides; FT-IR; <sup>1</sup>H and <sup>13</sup>C NMR; MALDI-TOF-MS; Mitogenic and comitogenic activity; Apoptosis; Phenolics

Xylo-oligosaccharides (XO) are a new group of oligosaccharides that are gaining importance as functional food ingredients<sup>1</sup> in pharmaceuticals, feed formulations, and agriculture.<sup>2</sup> XO exhibit excellent physicochemical and physiological properties. They act as prebiotics promoting the growth of beneficial bifidobacteria in the colon,<sup>3</sup> thus reducing the risk of colon cancer.<sup>4,5</sup> Long-chain XO have hypolipemic activity and improve intestinal function.<sup>6</sup> Glucuronic acid-containing XO show plant growth regulating activity<sup>7</sup> and antimicrobial activity.<sup>8</sup>

Besides the known physiological effects of various oligosaccharides,<sup>1,3</sup> immunopotentiating and apoptosis induction activities were reported for nigero- and agaro-oligosaccharides.<sup>1</sup> Our results represent a first report on the immunostimulatory activity of acetylated xylo-oligosaccharides, which in the case of the almond

shell XO comprise a mixture of neutral and acidic (4-O-methylglucuronic acid-containing) xylo-oligosaccharides, contaminated with very low amounts of phenolics. The immune system-potentiating activity as well as the presence of phenolics might support and contribute to further applications of the partially O-acetylated almond shell XO, isolated under autohydrolytic conditions.

For fragmentation of the xylan polymer, hydrothermal treatments with and without addition of acid, enzymic hydrolysis as well as their combinations were used.<sup>2,9–12</sup> Different separation processes were elaborated to obtain XO of the required purity from various agricultural and forest by-products, such as corncobs, various hardwood species, barley, oat spelt, etc.<sup>13,14</sup> Among the several xylan-rich biomass resources almond shells, produced in huge amounts (in Spain alone about  $2 \times 10^5$  ton per year), have a great potential for the production not only of xylose<sup>15</sup> but also of XO.

In an earlier study<sup>16</sup> it was shown that by controlling the temperature and time of the hydrothermal treatment

\* Corresponding author. Tel.: +34 977559652; fax: +34 977558544;  
e-mail: [deboranabarlatz@gmail.com](mailto:deboranabarlatz@gmail.com)

without addition of acid it is possible to influence the characteristics of XO obtained from almond shells, such as acetyl content, molecular mass, and purity. In a further study<sup>17</sup> autohydrolysis of almond shells was performed at 179 °C in a pilot scale reactor. The acetic acid resulting from hydrolysis of acetyl groups present in the hemicelluloses acts as a catalyst for the hydrolytic cleavage of xylan chains. The water-soluble product (SXO) recovered by spray-drying contained mainly XO with a broad molecular mass distribution aside from contaminating other carbohydrates, proteins, ash, various phenolics, and degradation products. Dialysis of SXO removed the monosaccharides and most of the shorter oligomers and other low-molecular weight substances, leaving in the retentate longer chain oligosaccharides (DXO) with a main molecular peak (84%) ~ 5000 Da. The carbohydrate composition analysis of both SXO and DXO (Table 1) revealed xylose to be the dominant sugar component. Its relative proportion increased after dialysis due to the loss of low-molecular weight fragments originating from carbohydrate (hexosans and pectic polysaccharides) and phenolic components.

The FT-IR spectra of SXO and DXO, shown in Figure 1, had similar patterns in the region 1200–1000  $\text{cm}^{-1}$ , typical of 4-*O*-methylglucuronoxylan xylan-type polysaccharides.<sup>18</sup> The absorption bands at ~1740  $\text{cm}^{-1}$  ( $\nu_{\text{C=O}}$ ) and ~1250  $\text{cm}^{-1}$  ( $\nu_{\text{C-O}}$ ) confirmed the presence of ester groups determined by chemical analysis.<sup>17</sup>

Solvent extraction was used to separate phenolics from the carbohydrate components of SXO. After re-dissolution of SXO in water, the insoluble part was separated by filtration and subsequently dissolved in methanol yielding the water-insoluble phenolic fraction, MeS. From the aqueous solution of SXO the water-soluble phenolic fraction, EAS, was phase-separated by ethyl acetate. The remaining aqueous phase yielded the purified XO (PuXO). As seen in Figure 1, the spectral pattern of MeS and EAS was similar and comprised mainly aromatic compounds.<sup>19</sup> This was evidenced by the absorption bands at 1710–1730, 1600–1605, and 1515  $\text{cm}^{-1}$  (aromatic ring and carbonyl groups), at 2965 and 2850  $\text{cm}^{-1}$  ( $\text{CH}_3$  and  $\text{CH}_2$  groups connected with aromatic structures) and at 834  $\text{cm}^{-1}$  (aromatic ring). However, weak xylo-oligosaccharide vibrations

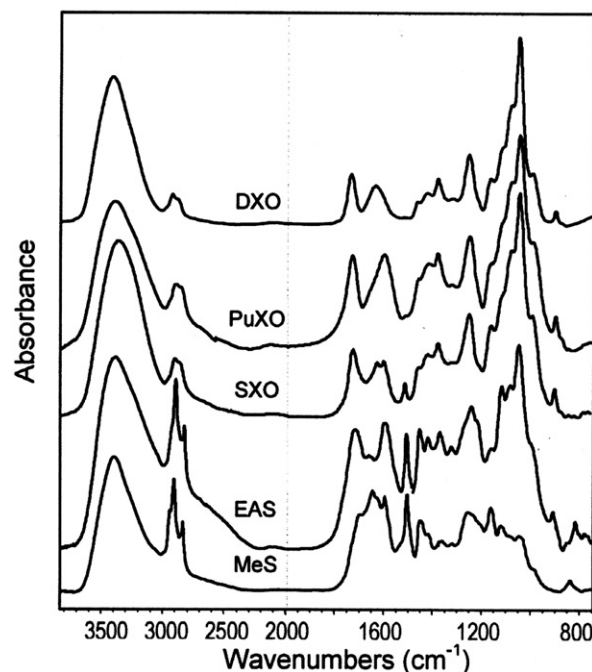


**Figure 1.** FT-IR spectra of the almond shell SXO and its purification products: DXO, after dialysis; MeS, methanol-soluble fraction; EAS, ethyl acetate soluble fraction; PuXO, purified fraction after ethyl acetate extraction.

were seen in the water-soluble phenolics (EAS). Both the spectra of DXO and PuXO were essentially the same, showing a very weak absorption at 1515  $\text{cm}^{-1}$ . The MeS and EAS fractions were separated also from DXO and their contents, determined gravimetrically, were 1.1% and 4.7%, respectively. The results suggest that most of the contaminating phenolics were removed by dialysis from SXO. They were mainly associated with the low-molecular weight substances accumulated in the diffusate, which might be used as a source of phenolics with potential antioxidant activity.<sup>20</sup>

The structural features of the almond shell oligosaccharides were examined by NMR spectroscopy of DXO and its de-acetylated form (DeXO). The chemical shifts of the signals observed in the  $^{13}\text{C}$  NMR spectra (in  $\text{D}_2\text{O}$ ) in Figure 2a and b, respectively, were in excellent agreement with values reported for various 4-*O*-methylglucuronoxylan oligomers and polymers, and their acetylated forms.<sup>21–23</sup> The relatively weak signals of

**Table 1.** Chemical characteristics of the crude (SXO) and dialyzed (DXO) oligosaccharides isolated from almond shells by autohydrolysis

Sample	Ash <sup>a</sup> (%)	Neutral sugar composition <sup>b</sup> (mol %)							MG <sup>c</sup> (%)	Ac (%)
		Rha	Fuc	Ara	Xyl	Man	Glc	Gal		
SXO	4.8	1.8	1.4	10.2	69.4	3.7	7.1	6.4	2.0	7.4 <sup>d</sup>
DXO	0	1.9	1.6	4.7	86.3	4.1	1.4	0	4.3	nd

<sup>a</sup> Residue after combustion at 850–900 °C.

<sup>b</sup> Sugars determined by GC of alditol trifluoroacetates after TFA hydrolysis.

<sup>c</sup> Content of 4-*O*-methylglucuronic acid (MG) as anhydro units, determined by potentiometry.

<sup>d</sup> *O*-Acetyl group content.<sup>17</sup>

the  $\alpha$ - and  $\beta$ -anomers of reducing Xylp end groups were in accordance with the average molecular mass ( $\sim 5000$  Da) of DXO,<sup>17</sup> confirming the presence of oligomeric and polymeric fragments. The xylan backbone of DXO contains acetyl groups at various positions and a rather low amount of 2-linked 4-*O*-methyl- $\alpha$ -D-glucuronic acid residue (MGA), which is in accordance with the data in Table 1. After de-acetylation (Fig. 2a), signals of the contaminating carbohydrates, such C-6 of Rhap at  $\delta$  17.9 and C-5 of Araf and C-6 of Galp at  $\delta$  62.2 and 61.6, respectively, were observed. The 2D-HSQC NMR spectrum of DXO (Fig. 3) showed  $^1\text{H}/^{13}\text{C}$  cross-peaks at  $\delta$  4.71/105.5 and 4.23/78.9, indicative of 4-linked  $\beta$ -Galp residues.<sup>24</sup>

The presence and location of acetyl groups was assigned from the anomeric region of the  $^1\text{H}$  NMR (not shown) and 2D-HSQC spectra of DXO (Fig. 3), which contain characteristic  $^1\text{H}/^{13}\text{C}$  cross-peaks of various structural elements (Table 2). The acetyl groups gave HSQC  $^1\text{H}/^{13}\text{C}$  cross-peaks at  $\delta$  2.22–2.10/22.0–20.7. In spite of the low MGA content, the cross-peaks of both MGA and the structural element XG3, corresponding to Xylp unit substituted at position 2 by MGA and acetylated at position 3, were detected. Similar results were reported for various O-acetylated hardwood glucuronoxylans<sup>22,23</sup> isolated by different extraction techniques. The cross-peaks depicted as  $\square$  in Figure 3 were not assigned because of a lack of further information. They might indicate the occurrence of various possible combinations of the presented structural elements.

The molar proportion of Xylp and MGA residues of DXO, calculated by integration of the corresponding H-1 signals areas, was 100:4.1. A similar ratio (100:4.8) was obtained by integration of the corresponding C-1 signals of the de-acetylated sample. The approximate average degree of substitution of the Xylp residues

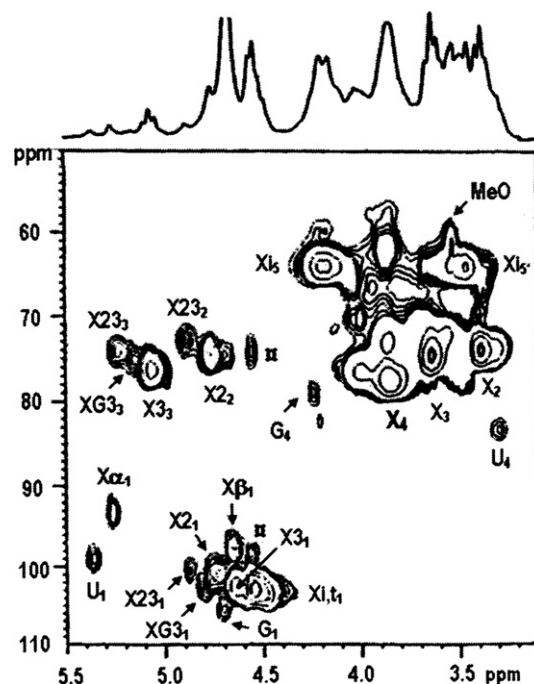


**Figure 3.** Partial  $^1\text{H}/^{13}\text{C}$  HSQC NMR spectrum (in  $\text{D}_2\text{O}$ ) of almond shell DXO. For designations of the cross-peaks see annotation in Table 1; G, 4-linked  $\beta$ -Galp. The subscript number corresponds to the respective H/C atom.

with acetyl groups, calculated<sup>23</sup> by integration of acetyl group signals (at  $\delta$  2.1–2.3) and of all carbohydrate proton signals, was 0.32. The distribution of acetyl groups in Xylp residues was determined<sup>22</sup> by integrating the areas of H-1 signals of internal, non-reducing and reducing terminal Xylp (Xint, Xt,  $\text{X}\alpha$ ,  $\text{X}\beta$ ), of the H-2 signal from 2-O-acetylated Xylp (X2), the H-3 signals from 3-O-acetylated Xylp (X3), 2,3-O-diacetylated Xylp (X23), and Xylp bearing the 2-linked MGA (XG3). The results

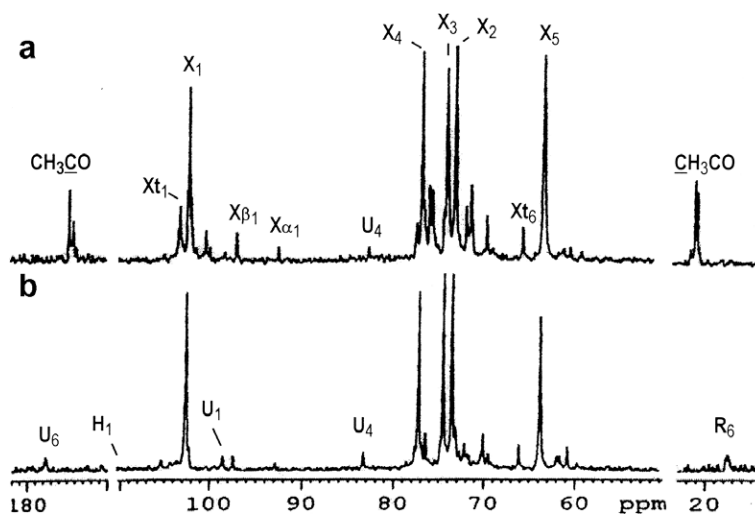


**Figure 2.**  $^{13}\text{C}$  NMR spectra (in  $\text{D}_2\text{O}$ ) of (a) acetylated xylo-oligosaccharides, DXO and (b) de-acetylated xylo-oligosaccharides, DeXO. X1–X5, internal Xylp, U, 4-*O*-methyl- $\alpha$ -glucuronic acid; H, hexopyranose; R, Rhap.

**Table 2.** HSQC NMR cross-peaks of various structural elements<sup>a</sup> of almond shell DXO

Element	Chemical shift <sup>1</sup> H/ <sup>13</sup> C (ppm)	Assignment
MG	5.34/98.4	H-1/C-1
X $\alpha$	5.26/93.5	H-1/C-1
X $\beta$	4.66/97.9	H-1/C-1
Xi, Xt	4.40–4.48/102.3–103.6	H-1/C-1
X2	4.75/100.9	H-1/C-1
	4.76/74.5	H-2/C-2
X3	4.54/102.6	H-1/C-1
	5.06/76.4	H-3/C-3
X23	4.87/100.3	H-1/C-1
	4.87/73.0	H-3/C-3
XG3	4.68/102.1	H-1/C-1
	5.16/75.0	H-3/C-3

<sup>a</sup> Designations used were: MG, 4-*O*-methylglucuronic acid; X $\alpha$  and X $\beta$ , Xylp reducing ends; Xi and Xt, Xylp internal and non-reducing terminal end; X2, 2-*O*-acetylated Xylp; X3, 3-*O*-acetylated Xylp; X23, 2,3-di-*O*-acetylated Xylp; XG3, MG 2-*O*-linked and 3-*O*-acetylated Xylp.

indicated that approximately 29% of the acetyl groups are located in position 2, 61% in position 3 including about 3% from XG3, and the rest (10%) in both positions.

Further analysis of the almond shell XO was performed by MALDI-TOF mass spectrometry of DXO and the de-acetylated sample, DeXO, which both contained more than 90% xylo-oligosaccharides. In accordance with this, the spectrum of DeXO (Fig. 4) showed a series of neutral xylo-oligosaccharides [X<sub>n</sub>] starting from X<sub>5</sub> and distinguishable up to X<sub>26</sub>; the higher oligomers were not discernible in the noise. A series of the expected acidic XO branched with one uronic acid [X<sub>n</sub>MGA] were detectable from X<sub>6</sub>MGA up to X<sub>18</sub>MGA. They show weaker intensities, and were separated from the two neighboring [X<sub>n</sub>] by 58 and 74 mass units, respectively (Fig. 4a). Also, some oligomers containing two MGA residues were detected, such as

X<sub>3</sub>MGA<sub>2</sub> (*m/z* 818) and X<sub>6</sub>MGA<sub>2</sub> (*m/z* 1213) up to X<sub>9</sub>MGA<sub>2</sub> (*m/z* 1609). Taking into account the MGA/X ratio of the DXO of about ~1:25, estimated by NMR spectroscopy, the distribution of the uronic acid side chains along the xylan chains seems to be blockwise rather than random. In the group of short XO (up to *m/z* 1000), in addition to X<sub>3</sub>, two acidic xylo-oligosaccharides are seen. They might be attributed to one containing a hexuronic acid unit, X<sub>3</sub>UA (*m/z* 613) and the second also a hexose unit, X<sub>2</sub>HUA (*m/z* 643).

A similar pattern in the region of the short XO was seen in the spectrum of DXO (Fig. 5). It showed a larger diversity of masses due to the presence of neutral xylo-oligomers with one to two acetyl groups [X<sub>n</sub>Ac<sub>m</sub>], clearly separated by 42 mass units, up to a DP 14 (Fig. 5a). The acidic XO containing one acetyl group, X<sub>2</sub>M<sub>2</sub> and X<sub>3</sub>M<sub>2</sub> with *m/z* 725 and 857, respectively, confirmed the presence of the XG3 structural element, detected by NMR spectroscopy.

The results of both the NMR spectroscopy and MALDI-TOF mass spectrometry analyses revealed that the almond shell xylo-oligosaccharides comprise a mixture of partially *O*-acetylated neutral and acidic oligomers derived from the 4-*O*-methylglucuronoxylan-type polymers, known to be the dominant hemicelluloses of dicotyl plants,<sup>25</sup> to which group the almond tree belongs.

The immunostimulatory activity was assessed using the comitogenic rat thymocyte test, which was proved to be applicable for polysaccharides of known immunomodulatory activities.<sup>26–28</sup> The test is based on the capacity of adjuvant immunomodulators to augment the proliferate response of rat thymocytes to T-mitogens in ‘vitro’. As illustrated in Table 3, the almond shell DXO showed dose-dependent direct mitogenic as well as comitogenic activities, as was the case with the immunogenic water-soluble arabinoglucuronoxylan from corncocks (CCX),<sup>28</sup> used as positive control. The activi-

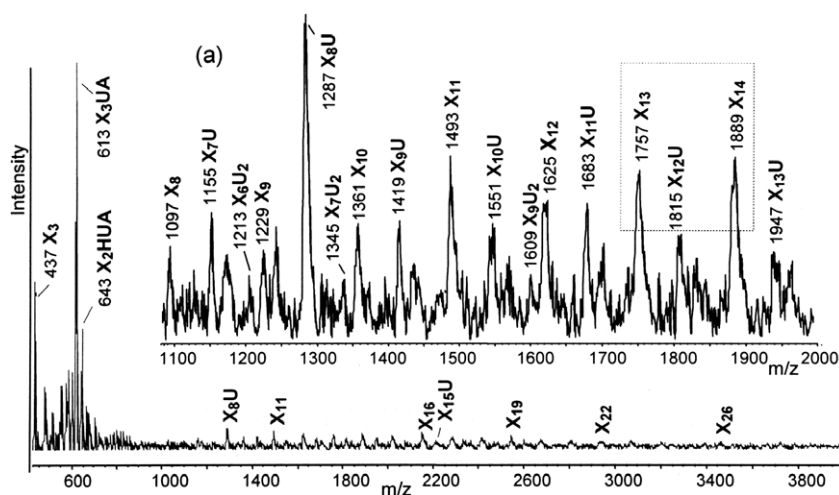


**Figure 4.** MALDI-TOF mass spectrum of the de-acetylated sample, DeXO (sodium-adducts). Inserted (a) is the extended region with *m/z* from 1000 to 2000 mass units. X = xylose; U = 4-*O*-methylglucuronic acid; UA, glucuronic or galacturonic acid; H, hexose.



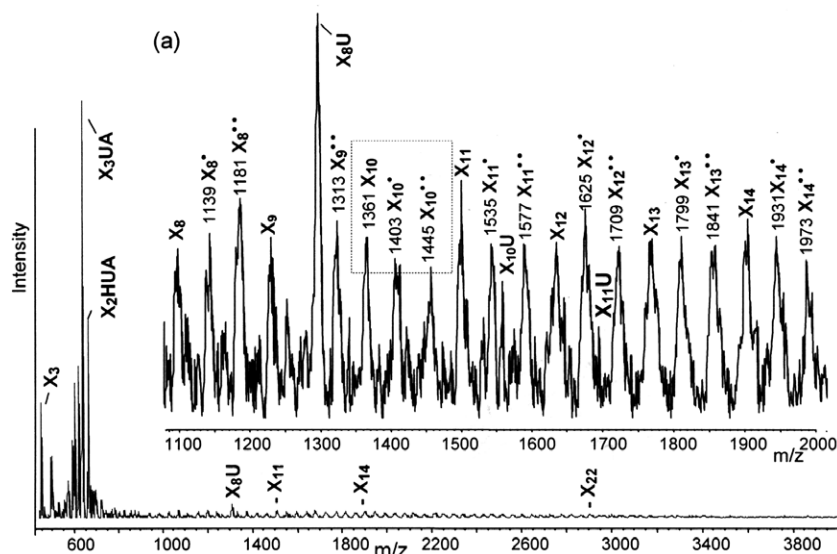


**Figure 5.** MALDI-TOF mass spectrum of O-acetylated xylo-oligosaccharides DXO (sodium-adducts). Inserted (a) is the extended region with  $m/z$  from 1000 to 2000 mass units. X = xylose; U = 4-*O*-methylglucuronic acid; UA, glucuronic or galacturonic acid; H, hexose; (●) = acetyl group.

**Table 3.** Mitogenic and comitogenic activities in vitro<sup>a</sup> of partially O-acetylated xylo-oligosaccharides from almond shells (AS-DXO) and corncobs (CC-DXO) in comparison to the corn cob xylan (CCX)<sup>28</sup> used as positive control

Sample	Stimulatory index, SI dose ( $\mu\text{g/mL}$ )				
	10	30	100	300	1000
<i>Mitogenic activity</i>					
AS-DXO	$0.9 \pm 0.1^a$	$1.2 \pm 0.1$	$1.5 \pm 0.3$	$4.6 \pm 0.9$	$18.5 \pm 6.5$
CC-DXO	$1.5 \pm 0.4$	$2.1 \pm 0.5$	$4.2 \pm 1.3$	$9.4 \pm 2.8$	$7.0 \pm 0.5$
CCX	$1.1 \pm 0.1$	$1.4 \pm 0.1$	$2.9 \pm 0.4$	$15.6 \pm 3.8$	$31.4 \pm 5.6$
<i>Comitogenic activity</i>					
AS-DXO	$1.1 \pm 0.2$	$1.2 \pm 0.1$	$2.0 \pm 0.2$	$10.4 \pm 4.2$	$39.7 \pm 17.4$
CC-DXO	$1.6 \pm 0.3$	$3.0 \pm 0.6$	$9.7 \pm 2.9$	$24.9 \pm 5.0$	$14.1 \pm 1.8$
CCX	$1.4 \pm 0.2$	$1.8 \pm 0.2$	$6.9 \pm 2.4$	$33.0 \pm 11.1$	$60.1 \pm 19.4$

The mean cpm for control cultures without any addition was 948 (704–1143). For cultures incubated with PHA, the mean cpm was 1331 (1081–1601).

<sup>a</sup> Results are represented as mean  $\pm$  SE based on four independent experiments.

ties in the whole doses range were about 30% lower in comparison to CCX. The  $\text{SI}_{\text{comit}}/\text{SI}_{\text{mit}}$  ratio of more than 2 indicates adjuvant properties.<sup>29</sup> For comparison, the xylo-oligosaccharides CC-DXO from corncobs,<sup>17</sup> which have the same 4-*O*-methylglucuronoxylan-type structure as the almond shell DXO, were tested as well. They also showed dose-dependent mitogenic and comitogenic activities increasing up to 300  $\mu\text{g/mL}$ , and decreasing at the highest applied dose. However, the immunostimulatory effect of CC-DXO was lower than that of CCX and AS-DXO.

## 1. Experimental

### 1.1. Material

The xylo-oligosaccharides (SXO) were prepared by spray-drying of the hydrolysis liquor obtained from almond shells by autohydrolysis at 179 °C for 23 min

in a pilot scale reactor and further dialyzed against distilled water yielding the dialyzed sample DXO.<sup>17</sup>

### 1.2. Analytical methods

The total hydrolysis of SXO and DXO was performed with 2 M TFA and the composition of neutral carbohydrates, separated by means of anion-exchange resin (Dowex 2  $\times$  8) from the hydrolyzate, was determined by GC analysis of the alditol trifluoroacetates using a Hewlett-Packard 5890 Series II chromatograph, as described in a previous paper.<sup>26</sup> The uronic acid content was determined by potentiometric titration of protonated samples.<sup>26</sup>

Fourier-transformed infrared (FT-IR) spectra (in KBr pellets) were obtained on a NICOLET Magna 750 spectrometer with a DTGS detector and OMNIC 3.2 software using 128 scans at a resolution of 4  $\text{cm}^{-1}$ . NMR spectra were recorded in  $\text{D}_2\text{O}$  at 27 and 60 °C on an FT NMR Bruker AVANCE DPX 300 spectrometer ( $^1\text{H}$  at

300.13 MHz and  $^{13}\text{C}$  at 75.46 MHz) equipped with a selective unit and gradient-enhanced spectroscopy kit (GRASP) for generation of  $z$ -gradients up to  $50\text{ G cm}^{-1}$  in a 5 mm inverse probe kit. Chemical shifts of signals were referenced to internal acetone (2.225 and 31.07 ppm for  $^1\text{H}$  and  $^{13}\text{C}$ , respectively). The data matrix for 2D-NMR experiments was processed with squared sine function, using Bruker software XWIN-NMR version 1.3.

The mass spectra were measured using the MALDI-TOF IV (Shimadzu, Kratos Analytical) instrument. Samples were irradiated by 337 nm photons from nitrogen laser. 2,5-Dihydroxybenzoic acid (DHB) was used as matrix. The samples (1 mg) were dissolved in 1 mL of an acetonitrile/water mixture (1:1, v/v). For the spot preparation, a mixture of 1  $\mu\text{L}$  of the matrix DHB with 10 pmol/ $\mu\text{L}$  analyte solution was used. Accelerating voltages applied for the MS measurements were 5 kV.

### 1.3. Procedure for the de-acetylation of DXO

DXO was subjected to de-acetylation with 0.1 M NaOH in the fridge overnight. After adjusting the pH 7 with 1 M HCl, the solution was dialyzed (Membra-Cel Dialysis Tubing, MWCO 3500 Da) and the retentate freeze-dried yielding sample DeXO.

### 1.4. Procedure for the solvent extraction

Samples (100 mg) of SXO and DXO were dissolved in distilled water (40 mL) under stirring for 2 h. The insoluble part separated by centrifugation at 10,000 rpm for 10 min was dissolved in MeOH yielding, after centrifugation of insoluble material and evaporation of the MeOH, fraction MeS. The aqueous supernatant was treated successively with three portions (20 mL) of ethyl acetate. The aqueous phase yielded after evaporation the purified fraction PuXO and the organic phase fraction EAS.

### 1.5. Immunostimulatory activity testing

The assay is based on the modified Iribe method<sup>29</sup> elaborated for muramyl glycopeptides, as described in more detail in a previous paper.<sup>26</sup> Rat thymocytes (Wistar strain, males weighting about 200 g) in RPMI-1640 medium supplemented with 5% fetal calf serum were cultivated at  $1.5 \times 10^6$  cells in 0.2 mL per well either without or with 25  $\mu\text{g/mL}$  of the T-mitogen, phytohaemagglutinin (PHA). Test compounds were added at final concentrations of 10, 30, 100, 300, and 1000  $\mu\text{g/mL}$ . After 72 h cultivation, thymocyte proliferation was measured by incorporation of  $^3\text{H}$ -thymidine, expressed in counts per minute (cpm). In each of four separate experiments, mean cpm for each set of four replicates were used to calculate the stimulation indices

(SI). The direct mitogenic activity was expressed as  $\text{SI}_{\text{mit}} = \text{mean cpm for test compound} / \text{mean cpm for the control without stimulant}$ . The comitogenic effect was expressed as  $\text{SI}_{\text{comit}} = \text{mean cpm (test compound + PHA)} / \text{mean cpm for PHA}$ . The mean cpm for control cultures without any addition was 948 (704–1143). For cultures incubated with PHA the mean cpm was 1331 (1081–1601). As positive control mitogenic corn cob xylan (CCX)<sup>28</sup> (produced in the Institute of Chemistry, SAS, Bratislava, Slovakia) was used. Possible contamination of the DXO with endotoxin was checked for in a parallel test performed in the presence of polymyxin B, which inhibits the biological effects of endotoxin including its mitogenic activity.<sup>26</sup> It was negative for the compounds tested.

### Acknowledgements

D. Montané is indebted to the Catalan Regional Government and the Spanish Government for financial support (Projects 2001SGR-00323 and PPQ2002-0421-CO2-02, respectively). D. Nabarlantz is obliged to the Catalan Regional Government (FI-IQUC) for her Ph.D. scholarship, and to the Chemical Engineering Department from the Rovira i Virgili University for the mobility scholarship. The Slovak grant Agency VEGA (Project No. 2/6131/06) and Slovak Academy of Sciences (Action Cost D28/006/03) are acknowledged for financial support, and Dr. V. Sasinková from the Institute of Chemistry for performing the FT-IR measurements.

### References

1. Nakakuki, T. *Trends Glycosci. Glycotechnol.* **2003**, *15*, 57–64.
2. Vazquez, M. J.; Alonso, J. L.; Domínguez, H.; Parajó, J. C. *Trends Food Sci. Technol.* **2000**, *11*, 387–393.
3. Crittenden, R.; Playne, M. *Trends Food Sci. Technol.* **1996**, *7*, 353–361.
4. Wollowski, I.; Rechkemmer, G.; Pool-Zobel, B. *Am. J. Clin. Nutr.* **2001**, *73*, 451–455.
5. Hsu, C. K.; Liao, J. W.; Chung, Y. C.; Hsieh, C. P.; Chan, Y. C. *J. Nutr.* **2004**, *134*, 1523–1528.
6. Izumo, Y.; Kojo A. Japan Patent 2003048901, 2003.
7. Nishihara, M.; Nagao, Y.; Shimizu, K. In *Proceedings of the 8th International Symposium on Wood and Pulp Chemistry, Helsinki*; 1995; Vol. 2, pp 17–22.
8. Christakopoulos, P.; Katapodis, P.; Kalogeris, E.; Kekos, D.; Macris, B. J.; Stamatis, H.; Skaltsa, H. *Int. J. Biol. Macromol.* **2003**, *31*, 171–175.
9. Kabel, M. A.; Schols, H. A.; Voragen, A. G. J. *Carbohydr. Polym.* **2002**, *50*, 191–200.
10. Nabarlantz, D.; Farriol, X.; Montané, D. *Ind. Eng. Chem. Res.* **2004**, *43*, 4124–4131.
11. Pellerin, P.; Gosselin, M.; Lepoutre, J.-R.; Samain, E.; Debeire, P. *Enzyme Microb. Technol.* **1991**, *13*, 617–621.

12. Yang, R.; Xu, S.; Wang, Z.; Wang, M. *LWT-Food Sci. Technol.* **2005**, *38*, 677–682.
13. Vegas, R.; Alonso, J. L.; Domínguez, H.; Parajó, J. C. *Ind. Eng. Chem. Res.* **2005**, *44*, 614–620.
14. Montané, D.; Nabarlitz, D.; Martorell, A.; Torné-Fernández, V.; Fierro, V. *Ind. Eng. Chem. Res.* **2006**, *45*, 2294–2302.
15. Pou-Ilías, J.; Canellas, J.; Driguez, H.; Excoffier, G.; Vignon, M. R. *Carbohydr. Res.* **1990**, *207*, 126–130.
16. Nabarlitz, D.; Farriol, X.; Montané, D. *Ind. Eng. Chem. Res.* **2005**, *44*, 7746–7755.
17. Nabarlitz, D.; Ebringerová, A.; Montané, D. *Carbohydr. Polym.*, in press, doi:10.1016/j.carbpol.2006.08.020.
18. Kačuráková, M.; Capek, P.; Sasinková, V.; Wellner, K.; Ebringerová, A. *Carbohydr. Polym.* **2000**, *43*, 195–203.
19. Faix, O. *Holzforschung* **1991**, *45*, 21–27.
20. Garrote, G.; Cruz, J. M.; Domínguez, H.; Parajó, J. C. *J. Chem. Technol. Biotechnol.* **2003**, *78*, 392–398.
21. Kardošová, A.; Matulová, M.; Malovíková, A. *Carbohydr. Res.* **1998**, *308*, 99–106.
22. Teleman, A.; Lundqvist, J.; Tjerneld, F.; Stålbrand, H.; Dahlman, O. *Carbohydr. Res.* **2000**, *329*, 807–815.
23. Teleman, A.; Tenkanen, M.; Jacobs, A.; Dahlman, O. *Carbohydr. Res.* **2002**, *337*, 373–377.
24. Morris, G.; Hromádková, Z.; Ebringerová, A.; Malovíková, A.; Alföldi, J.; Harding, S. E. *Carbohydr. Polym.* **2002**, *48*, 351–359.
25. Ebringerová, A.; Heinze, T. *Macromol. Rapid Commun.* **2000**, *21*, 542–556.
26. Ebringerová, A.; Kardošová, A.; Hromádková, Z.; Malovíková, A.; Hříbalová, V. *Int. J. Biol. Macromol.* **2002**, *30*, 1–6.
27. Rovenský, J.; Pekárek, J.; Mlynářčík, D.; Kasářík, E.; Lackovič, V.; Hříbalová, V.; Buc, M. In *Immunology: Clinical, Fundamental and Therapeutic Aspects*; Ram, B. P., Harris, M. C., Tyle, P., Eds.; VCH: New York, 1990; pp 344–354.
28. Ebringerová, A.; Hromádková, Z.; Hříbalová, V. *Int. J. Biol. Macromol.* **1995**, *17*, 327–332.
29. Iribe, H.; Koba, T. *Cell Immunol.* **1984**, *88*, 9–15.